Physics Letters B 713 (2012) 378–386

Contents lists available at SciVerse ScienceDirect

Physics Letters B

www.elsevier.com/locate/physletb

Measurement of the *CP*-violating phase ϕ_s in $\overline{B}{}^0_s \to J/\psi\pi^+\pi^-$ decays ☆

LHCb Collaboration

ARTICLE INFO

Article history:
Received 26 April 2012
Received in revised form 23 May 2012
Accepted 12 June 2012
Available online 15 June 2012
Editor: W.-D. Schlatter

ABSTRACT

Measurement of the mixing-induced *CP*-violating phase ϕ_s in $\overline{B}{}^0_s$ decays is of prime importance in probing new physics. Here 7421 ± 105 signal events from the dominantly *CP*-odd final state $J/\psi\pi^+\pi^-$ are selected in 1 fb^{-1} of pp collision data collected at $\sqrt{s} = 7$ TeV with the LHCb detector. A time-dependent fit to the data yields a value of $\phi_s = -0.019^{+0.173+0.004}_{-0.174-0.003}$ rad, consistent with the Standard Model expectation. No evidence of direct *CP* violation is found.

1. Introduction

Current knowledge of the Cabibbo–Kobayashi–Maskawa (CKM) matrix leads to the Standard Model (SM) expectation that the mixing-induced *CP* violation phase in $\overline{B}{}^0_s$ decays proceeding via the $b \to c\bar{c}s$ transition is small and accurately predicted [1]. Therefore, new physics can be decisively revealed by its measurement. This phase denoted by ϕ_s is given in the SM by $-2\arg[V_{ts}V^*_{tb}/V_{cs}V^*_{cb}]$, where the V_{ij} are elements of the CKM matrix. Motivated by a prediction in Ref. [2], the LHCb Collaboration made the first observation of $\overline{B}{}^0_s \to J/\psi f_0(980)$, $f_0(980) \to \pi^+\pi^-$ [3], which was subsequently confirmed by others [4,5]. This mode is a *CP*-odd eigenstate and its use obviates the need to perform an angular analysis in order to determine ϕ_s [6], as is required in the $J/\psi\phi$ final state [7,8]. In this Letter we measure ϕ_s using the final state $J/\psi\pi^+\pi^-$ over a large range of $\pi^+\pi^-$ masses, 775–1550 MeV,[1] which has been shown to be an almost pure *CP*-odd eigenstate [9]. We designate events in this region as $f_{\rm odd}$. This phase is the same as that measured in $J/\psi\phi$ decays, ignoring contributions from suppressed processes [10].

The decay time evolutions for initial B^0_s and $\overline{B}{}^0_s$ decaying into a *CP*-odd eigenstate, f_-, assuming only one CKM phase, are [11]

$$\begin{aligned}&\Gamma\big(\overset{(-)}{B}{}^0_s \to f_-\big)\\ &= \mathcal{N} e^{-\Gamma_s t}\left\{\frac{e^{\Delta\Gamma_s t/2}}{2}(1+\cos\phi_s)\right.\\ &\quad\left.+\frac{e^{-\Delta\Gamma_s t/2}}{2}(1-\cos\phi_s) \pm \sin\phi_s \sin(\Delta m_s t)\right\},\end{aligned} \tag{1}$$

where $\Delta\Gamma_s = \Gamma_{\rm L} - \Gamma_{\rm H}$ is the decay width difference between light and heavy mass eigenstates, $\Gamma_s = (\Gamma_{\rm L} + \Gamma_{\rm H})/2$ is the average decay width, $\Delta m_s = m_{\rm H} - m_{\rm L}$ is the mass difference, and $\mathcal{N}$ is a time-independent normalization factor. The plus sign in front of the $\sin\phi_s$ term applies to an initial $\overline{B}{}^0_s$ and the minus sign to an initial B^0_s meson. The time evolution of the untagged rate is then

$$\begin{aligned}&\Gamma\big(B^0_s \to f_-\big) + \Gamma\big(\overline{B}{}^0_s \to f_-\big)\\ &= \mathcal{N} e^{-\Gamma_s t}\left\{e^{\Delta\Gamma_s t/2}(1+\cos\phi_s) + e^{-\Delta\Gamma_s t/2}(1-\cos\phi_s)\right\}.\end{aligned} \tag{2}$$

Note that there is information in the shape of the lifetime distribution that correlates $\Delta\Gamma_s$ and ϕ_s. In this analysis we will use samples of both flavor tagged and untagged decays. Both Eqs. (1) and (2) are invariant under the change $\phi_s \to \pi - \phi_s$ when $\Delta\Gamma_s \to -\Delta\Gamma_s$, which gives an inherent ambiguity. Recently this ambiguity has been resolved [12], so only the allowed solution with $\Delta\Gamma_s > 0$ will be considered.

2. Data sample and selection requirements

The data sample consists of 1 fb^{-1} of integrated luminosity collected with the LHCb detector [13] at 7 TeV centre-of-mass energy in pp collisions at the LHC. The detector is a single-arm forward spectrometer covering the pseudorapidity range $2 < \eta < 5$, designed for the study of particles containing b or c quarks. Components include a high-precision tracking system consisting of a silicon-strip vertex detector surrounding the pp interaction region, a large-area silicon-strip detector located upstream of a dipole magnet with a bending power of about 4 Tm, and three stations of silicon-strip detectors and straw drift-tubes placed downstream. The combined tracking system has a momentum resolution $\delta p/p$ that varies from 0.4% at 5 GeV to 0.6% at 100 GeV, and an impact parameter (IP) resolution of 20 μm for tracks with high transverse momentum ($p_{\rm T}$). Charged hadrons are identified using two ring-imaging Cherenkov (RICH) detectors. Photon, electron and hadron candidates are identified by a calorimeter system consisting of scintillating-pad and pre-shower detectors, an electromagnetic calorimeter and a hadronic calorimeter. Muons are identified by a muon system composed of alternating layers of iron and multiwire

☆ © CERN for the benefit of the LHCb Collaboration.

[1] We work in units where $c = \hbar = 1$.

0370-2693/
http://dx.doi.org/10.1016/j.physletb.2012.06.032

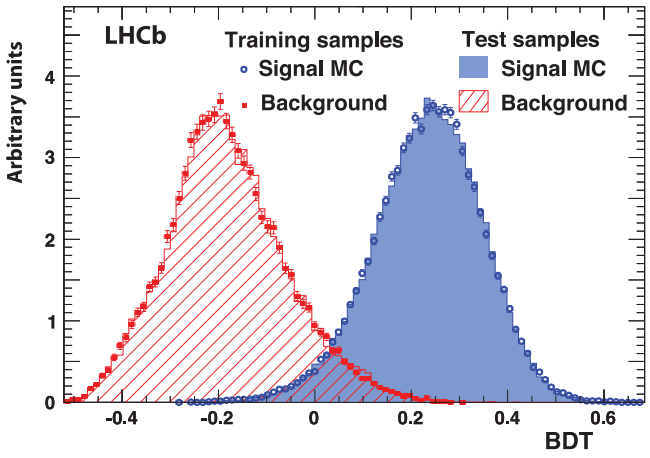

Fig. 1. Distributions of the BDT variable for both training and test samples of $J/\psi\pi\pi$ signal and background events. The signal samples are from simulation and the background samples derived from data. (For interpretation of the references to color in this figure, the reader is referred to the web version of this Letter.)

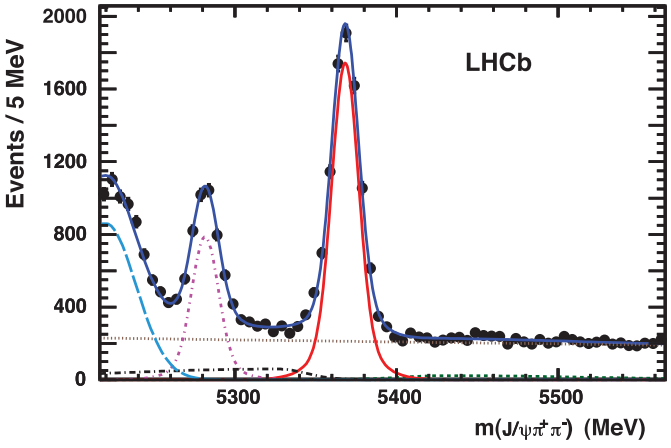

Fig. 2. Mass distribution of the selected $J/\psi\pi^+\pi^-$ combinations in the $f_{\rm odd}$ region. The blue solid curve shows the result of a fit with a double Gaussian signal (red solid curve) and several background components: combinatorial background (brown dotted line), background from $B^- \to J/\psi K^-$ and $J/\psi\pi^-$ (green short-dashed line), $\overline{B}^0 \to J/\psi\pi^+\pi^-$ (purple dot-dashed), $\overline{B}^0_s \to J/\psi\eta'$ and $\overline{B}^0_s \to J/\psi\phi$ when $\phi \to \pi^+\pi^-\pi^0$ (black dot-long-dashed), and $\overline{B}^0 \to J/\psi K^-\pi^+$ (light-blue long-dashed). (For interpretation of the references to color in this figure, the reader is referred to the web version of this Letter.)

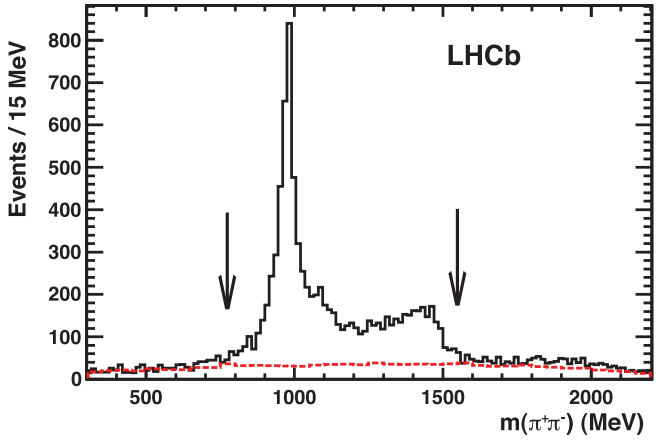

Fig. 3. Mass distribution of selected $\pi^+\pi^-$ combinations shown as the (solid black) histogram for events in the $\overline{B}^0_s$ signal region. The (dashed red) line shows the background determined by fitting the $J/\psi\pi^+\pi^-$ mass in bins of $\pi^+\pi^-$ mass. The arrows designate the limits of the $f_{\rm odd}$ region. (For interpretation of the references to color in this figure, the reader is referred to the web version of this Letter.)

proportional chambers. The trigger consists of a hardware stage, based on information from the calorimeter and muon systems, followed by a software stage which applies a full event reconstruction.

Events were triggered by detecting two muons with an invariant mass within 120 MeV of the nominal J/ψ mass [14]. To be considered a J/ψ candidate, particles of opposite charge are required to have $p_{\rm T}$ greater than 500 MeV, be identified as muons, and form a vertex with fit χ^2 per number of degrees of freedom less than 16. Only candidates with a dimuon invariant mass between -48 MeV and $+43$ MeV of the J/ψ mass peak are selected. For further analysis the four-momenta of the dimuons are constrained to yield the J/ψ mass.

For this analysis we use a Boosted Decision Tree (BDT) [15] to set the $J/\psi\pi^+\pi^-$ selection requirements. We first implement a preselection that preserves a large fraction of the signal events, including the requirements that the pions have $p_{\rm T} > 250$ MeV and be identified by the RICH. $\overline{B}^0_s$ candidate decay tracks must form a common vertex that is detached from the primary vertex. The angle between the combined momentum vector of the decay products and the vector formed from the positions of the primary and the $\overline{B}^0_s$ decay vertices (pointing angle) is required to be consistent with zero. If more than one primary vertex is found the one corresponding to the smallest IP significance of the $\overline{B}^0_s$ candidate is chosen.

The variables used in the BDT are the muon identification quality, the probability that the $\pi^\pm$ come from the primary vertex (implemented in terms of the IP χ^2), the $p_{\rm T}$ of each pion, the $\overline{B}^0_s$ vertex χ^2, the pointing angle and the $\overline{B}^0_s$ flight distance from production to decay vertex. For various calibrations we also analyze samples of $\overline{B}^0 \to J/\psi\overline{K}^{*0}$, $\overline{K}^{*0} \to \pi^+K^-$, and its charge-conjugate. The same selections are used as for $J/\psi\pi^+\pi^-$ except for particle identification.

The BDT is trained with $\overline{B}^0_s \to J/\psi f_0(980)$ Monte Carlo events generated using Pythia [16] and the LHCb detector simulation based on Geant4 [17]. The following two data samples are used to study the background. The first contains $J/\psi\pi^+\pi^+$ and $J/\psi\pi^-\pi^-$ events with $m(J/\psi\pi^\pm\pi^\pm)$ within ± 50 MeV of the $\overline{B}^0_s$ mass, called the like-sign sample. The second consists of events in the $\overline{B}^0_s$ sideband having $m(J/\psi\pi^+\pi^-)$ between 200 and 250 MeV above the $\overline{B}^0_s$ mass peak. In both cases we require $775 < m(\pi\pi) < 1550$ MeV.

Separate samples are used to train and test the BDT. Training samples consist of 74,230 signal and 31,508 background events, while the testing samples contain 74,100 signal and 21,100 background events. Fig. 1 shows the signal and background BDT distributions of the training and test samples. The training and test samples are in excellent agreement. We select $\overline{B}^0_s \to J/\psi\pi^+\pi^-$ candidates with BDT > 0 to maximize signal significance for further analysis.

The $J/\psi\pi^+\pi^-$ mass distribution is shown in Fig. 2 for the $f_{\rm odd}$ region. In the $\overline{B}^0_s$ signal region, defined as ± 20 MeV around the $\overline{B}^0_s$ mass peak, there are 7421 ± 105 signal events, 1717 ± 38 combinatorial background events, and 66 ± 9 η' background events, corresponding to an 81% signal purity. The $\pi^+\pi^-$ mass distribution is shown in Fig. 3. The most prominent feature is the $f_0(980)$, containing 52% of the events within ± 90 MeV of 980 MeV, called the f_0 region. The rest of the $f_{\rm odd}$ region is denoted as $\tilde{f}_0$.

3. Resonance structure in the $J/\psi\pi^+\pi^-$ final state

The resonance structure in $\overline{B}^0_s \to J/\psi\pi^+\pi^-$ decays has been studied using a modified Dalitz plot analysis including the de-

Table 1
Resonance fractions in $\overline{B}{}^0_s \to J/\psi\pi^+\pi^-$ over the full mass range [9]. The final-state helicity of the D-wave is denoted by Λ. Only statistical uncertainties are quoted.

Resonance	Normalized fraction (%)
$f_0(980)$	69.7 ± 2.3
$f_0(1370)$	21.2 ± 2.7
non-resonant $\pi^+\pi^-$	8.4 ± 1.5
$f_2(1270)$, $\Lambda = 0$	0.49 ± 0.16
$f_2(1270)$, $\lvert\Lambda\rvert = 1$	0.21 ± 0.65

cay angular distribution of the J/ψ meson [9]. A fit is performed to the decay distributions of several $\pi^+\pi^-$ resonant states described by interfering decay amplitudes. The largest component is the $f_0(980)$ that is described by a Flatté function [18]. The data are best described by adding Breit–Wigner amplitudes for the $f_0(1370)$ and $f_2(1270)$ resonances and a non-resonant amplitude. The components and fractions of the best fit are given in Table 1.

The final state is dominated by *CP*-odd S-wave over the entire $f_{\rm odd}$ region. We also have a small D-wave component associated with the $f_2(1270)$ resonance. Its zero helicity ($\Lambda = 0$) part is also pure *CP*-odd and corresponds to $(0.49 \pm 0.16^{+0.02}_{-0.08})\%$ of the total rate.[2] The $|\Lambda| = 1$ part, which is of mixed *CP*, corresponds to $(0.21 \pm 0.65^{+0.01}_{-0.03})\%$ of the total. Performing a separate fit, we find that a possible ρ contribution is smaller than 1.5% at 95% confidence level (CL). Summing the $f_2(1270)$ $|\Lambda| = 1$ and ρ rates, we find that the *CP*-odd fraction is larger than 0.977 at 95% CL. Thus the entire mass range can be used to study *CP* violation in this almost pure *CP*-odd final state.

4. Flavor tagging

Knowledge of the initial $\overline{B}{}^0_s$ flavor is necessary in order to use Eq. (1). This is realized by tagging the flavor of the other b hadron in the event, exploiting information from four sources: the charges of muons, electrons, kaons with significant IP, and inclusively reconstructed secondary vertices. The decisions of the four tagging algorithms are individually calibrated using $B^\mp \to J/\psi K^\mp$ decays and combined using a neural network as described in Ref. [19]. The tagging performance is characterized by $\varepsilon_{\rm tag} D^2$, where $\varepsilon_{\rm tag}$ is the efficiency and D the dilution, defined as $D \equiv (1 - 2\omega)$, where ω is the probability of an incorrect tagging decision.

We use both the information of the tag decision and of the predicted per-event mistag probability. The calibration procedure assumes a linear dependence between the predicted mistag probability η_i for each event and the actual mistag probability ω_i given by $\omega_i = p_0 + p_1 \cdot (\eta_i - \langle\eta\rangle)$, where p_0 and p_1 are calibration parameters and $\langle\eta\rangle$ the average estimated mistag probability as determined from the $J/\psi K^\mp$ calibration sample. The values are $p_0 = 0.392 \pm 0.002 \pm 0.009$, $p_1 = 1.035 \pm 0.021 \pm 0.012$, and $\langle\eta\rangle = 0.391$. Systematic uncertainties are evaluated by using $J/\psi K^+$ separately from $J/\psi K^-$, performing the calibration with $\overline{B}{}^0 \to J/\psi \overline{K}{}^{*0}$ and $\overline{B}{}^0 \to D^{*+}\mu^-\overline{\nu}_\mu$ plus charge-conjugate channels, and viewing the dependence on different data taking periods. We find $\varepsilon_{\rm tag} = (32.9 \pm 0.6)\%$ providing us with 2445 tagged signal events. The dilution is measured as $D = 0.272 \pm 0.004 \pm 0.015$, leading to $\varepsilon_{\rm tag} D^2 = (2.43 \pm 0.08 \pm 0.26)\%$.

5. Decay time resolution

The $\overline{B}{}^0_s$ decay time is defined here as $t = m\vec{d} \cdot \vec{p}/|p|^2$, where m is the reconstructed invariant mass, $\vec{p}$ the momentum and $\vec{d}$ the vector from the primary to the secondary vertex. The time resolution for signal increases by about 20% for decay times from 0 to 10 ps, according to both the simulation and the estimate of the resolution from the reconstruction. To take this dependence into account, we use a double-Gaussian resolution function with widths proportional to the event-by-event estimated resolution,

$$T(t - \hat{t}; \sigma_t) = \sum_{i=1}^{2} f_i^T \frac{1}{\sqrt{2\pi} S_i \sigma_t} e^{-\frac{(t-\hat{t}-\mu_t)^2}{2(S_i\sigma_t)^2}}, \qquad (3)$$

where $\hat{t}$ is the true time, σ_t the estimated time resolution, μ_t is the bias on the time measurement, $f_1^T + f_2^T = 1$ are the fractions of each Gaussian, and S_1 and S_2 are scale factors.

To determine the parameters of T we use events containing a J/ψ, found using a dimuon trigger without track impact pa-

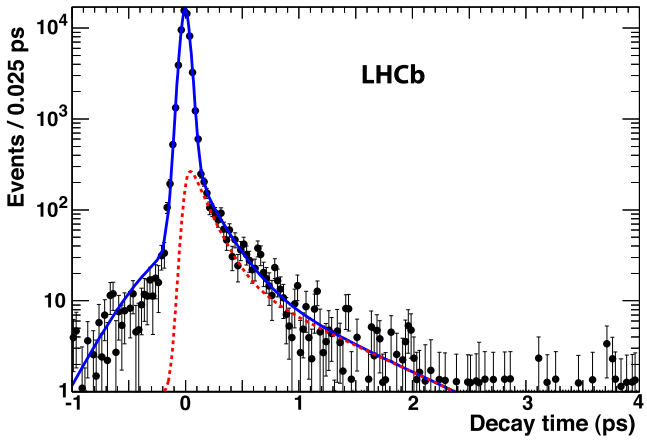

Fig. 4. Decay time distribution of prompt $J/\psi\pi^+\pi^-$ candidates in the f_0 region. The dashed (red) line shows the long-lived component, and the solid curve the total. (For interpretation of the references to color in this figure, the reader is referred to the web version of this Letter.)

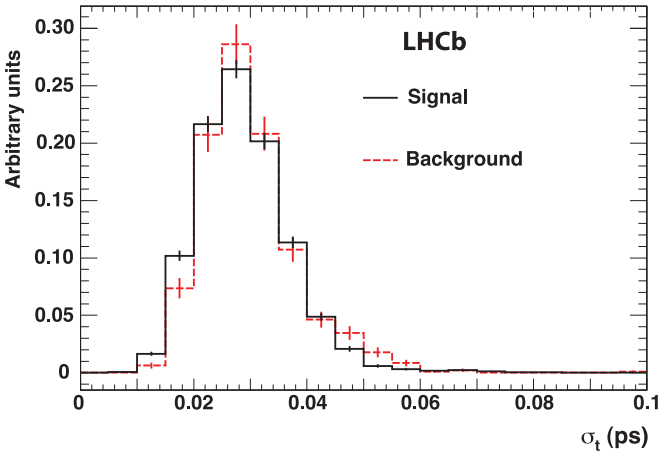

Fig. 5. Distribution of the estimated time resolution σ_t for opposite-sign $J/\psi\pi^+\pi^-$ signal events after background subtraction, and for like-sign background.

Table 2
Parameters of the decay time resolution function determined from fits to $J/\psi\pi^+\pi^-$ prompt data samples.

Parameter	f_0 region	$\bar{f}_0$ region
μ_t (fs)	−3.32(12)	−2.91(7)
S_1	1.362(4)	1.329(2)
S_2	12.969(3)	9.108(3)
f_2^T	0.0193(7)	0.0226(5)

[2] In this Letter whenever two uncertainties are given, the first is statistical and the second systematic.

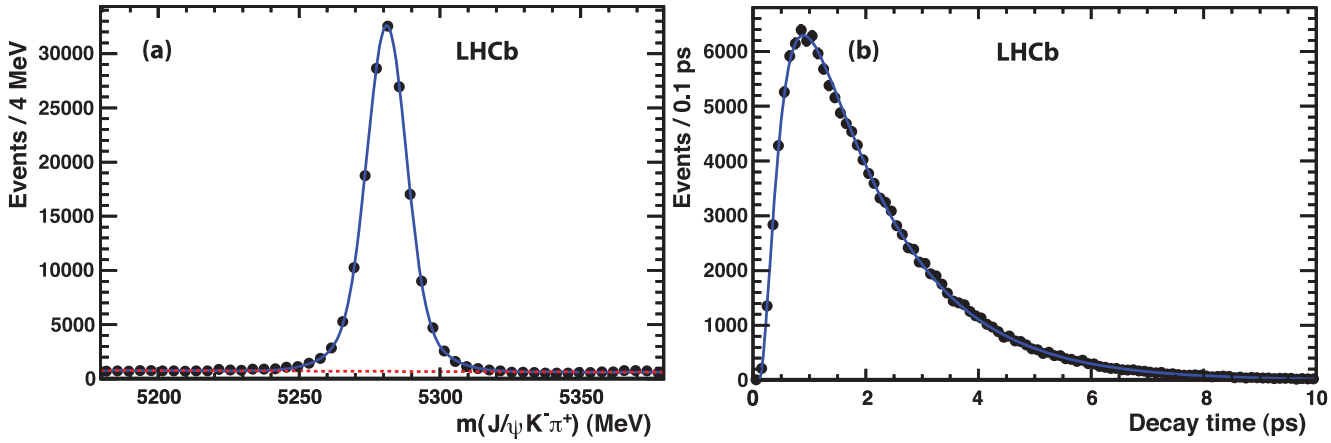

Fig. 6. (a) Mass distribution of $\overline{B}^0 \to J/\psi \overline{K}^{*0}$ candidates. The dashed (red) line shows the background, and the solid (blue) curve the total. (b) Decay time distribution, where the small background has been subtracted using the $\overline{B}^0$ mass sidebands. The (blue) curve shows the lifetime fit. (For interpretation of the references to color in this figure, the reader is referred to the web version of this Letter.)

rameter requirements, plus two opposite-sign charged tracks with similar selection criteria as for $J/\psi\pi^+\pi^-$ events including that the $J/\psi\pi^+\pi^-$ mass be within ±20 MeV of the $\overline{B}_s^0$ mass. Fig. 4 shows the decay time distribution for this $J/\psi\pi^+\pi^-$ prompt data sample for the f_0 region; the $\tilde{f}_0$ data are very similar. The data are fitted with the time dependence given by

$$P^{\text{prompt}}(t) = (1 - f_1 - f_2)T(t;\sigma_t) + \left[\frac{f_1}{\tau_1}e^{-\hat{t}/\tau_1} + \frac{f_2}{\tau_2}e^{-\hat{t}/\tau_2}\right] \otimes T(t-\hat{t};\sigma_t), \quad (4)$$

where f_1 and f_2 are long-lived background fractions with lifetimes τ_1 and τ_2, respectively. The resulting parameter values of the function T are given in Table 2.

Fig. 5 shows the σ_t distributions used in Eq. (3) for $J/\psi\pi^+\pi^-$ events in the f_{odd} region after background subtraction, and for like-sign background. Taking into account the calibration parameters of Table 2, the average effective decay time resolution for the signal is 40.2 fs and 39.3 fs for the f_0 and $\tilde{f}_0$ regions, respectively. The average of the two samples is 39.8 fs.

6. Decay time acceptance

The decay time acceptance function is written as

$$A(t;a,n,t_0) = C\frac{[a(t-t_0)]^n}{1+[a(t-t_0)]^n}, \quad (5)$$

where C is a normalization constant. The other parameters are determined by fitting the lifetime distribution of $\overline{B}^0 \to J/\psi\overline{K}^{*0}$ events, where $\overline{K}^{*0} \to K^-\pi^+$. Fig. 6(a) shows the $J/\psi\overline{K}^{*0}$ mass when the $K^-\pi^+$ invariant mass is within ±300 MeV of 892 MeV. There are 155,743 ± 434 signal events. The sideband-subtracted decay time distribution is shown in Fig. 6(b) together with a lifetime fit taking into account the acceptance and resolution. This fit yields $a = 2.11 \pm 0.04$ ps^{-1}, $n = 1.82 \pm 0.06$, $t_0 = 0.105 \pm 0.006$ ps and a lifetime of 1.516 ± 0.008 ps, in good agreement with the PDG average of 1.519 ± 0.007 ps [14].

We check our lifetime acceptance by comparing with a CDF measurement of the $\overline{B}_s^0 \to J/\psi f_0$ effective lifetime of $\tau^{\text{eff}} = 1.70^{+0.12}_{-0.11} \pm 0.03$ ps [5] obtained from a single exponential fit.[3] A fit of the f_0 sample (see Fig. 7) yields $\tau^{\text{eff}} = 1.71 \pm 0.03$ ps, while we find $\tau^{\text{eff}} = 1.67 \pm 0.03$ ps in the $\tilde{f}_0$ sample. These two values are consistent with each other, within the quoted statistical errors, and with the CDF result.

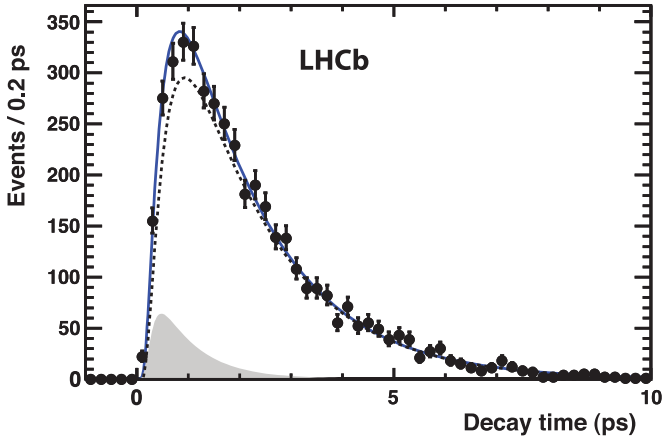

Fig. 7. Decay time distribution of $\overline{B}_s^0 \to J/\psi f_0$ candidates fitted with a single exponential function multiplied by the acceptance and convolved with the resolution. The dashed line is signal and the shaded area background.

7. Likelihood function definition

To determine ϕ_s an extended likelihood function is maximized using candidates in the $\overline{B}_s^0$ signal region

$$\mathcal{L}(\phi_s) = e^{-(N_{\text{sig}}+N_{\text{bkg}})}\prod_{i=1}^{N_{\text{obs}}} P(m_i, t_i, \sigma_{ti}, q_i, \eta_i), \quad (6)$$

where the signal yield, N_{sig}, and background yield, N_{bkg}, are fixed from the fit of the $J/\psi\pi^+\pi^-$ mass distribution in the f_{odd} region (see Fig. 2). N_{obs} is the number of $\overline{B}_s^0$ candidates, m_i the reconstructed mass, t_i the reconstructed decay time, and σ_{ti} the estimated decay time uncertainty. The flavor tag, q_i, takes values of +1, −1 or 0, respectively, if the signal meson is tagged as B_s^0, $\overline{B}_s^0$, or untagged, and η_i is the estimated mistag probability. Backgrounds are caused largely by mis-reconstructed b-hadron decays, so it is necessary to include a long-lived background probability density function (PDF). The likelihood function includes dis-

[3] This corresponds to the lifetime of the CP-odd eigenstate if ϕ_s is zero (see Eq. (2)).

Table 3
Parameters used in the functions for the invariant mass and decay time describing the signal and background. These parameters are fixed to their central values in the fit for ϕ_s.

Function	Parameters
	$N_{\rm sig} = 7421$, $N_{\rm bkg} = 1717 \pm 38$, $N_{\eta'} = 66 \pm 9$
$P_m^{\rm sig}(m)$	$m_0 = 5368.2(1)$ MeV, $\sigma_1^m = 8.1(1)$ MeV, $\sigma_2^m = 18.0(2)$ MeV, $f_2^m = 0.196(2)$
$P_m^{\rm bkg}(m)$	$\alpha = (-5.35 \pm 1.15) \times 10^{-4}$ MeV^{-1}
$P_t^{\rm bkg}(t\|\sigma_t)$	$\tau_1^{\rm bkg} = 0.65(5)$ ps, $\tau_2^{\rm bkg} = 2.0(8)$ ps, $f_2^{\rm bkg} = 0.06(2)$
$T(t-\hat{t};\sigma_t)$	$a^{\rm bkg} = 3.22(10)$ ps^{-1}, $n^{\rm bkg} = 3.31(14)$, $t_0^{\rm bkg} = 0$ ps, see Table 2

tinct contributions from the signal and the background. For tagged events we have

$$\begin{aligned} &P(m_i, t_i, \sigma_{ti}, q_i, \eta_i) \\ &\quad = N_{\rm sig}\varepsilon_{\rm tag} P_m^{\rm sig}(m_i) P_t^{\rm sig}(t_i, q_i, \eta_i|\sigma_{ti}) P_{\sigma_t}^{\rm sig}(\sigma_{ti}) \\ &\quad + N_{\rm bkg}\varepsilon_{\rm tag}^{\rm bkg} P_m^{\rm bkg}(m_i) P_t^{\rm bkg}(t_i|\sigma_{ti}) P_{\sigma_t}^{\rm bkg}(\sigma_{ti}), \end{aligned} \tag{7}$$

where $\varepsilon_{\rm tag}^{\rm bkg}$ refers to the flavor tagging efficiency of the background. The signal mass PDF, $P_m^{\rm sig}(m)$, is a double Gaussian function, while the background mass PDF, $P_m^{\rm bkg}(m)$, is proportional to $e^{-\alpha m}$ together with a very small contribution from $\overline{B}{}_s^0 \to J/\psi\eta'$, $N_{\eta'}$, that is fixed in the ϕ_s fit to 66 events obtained from the fit shown in Fig. 2.

The PDF used to describe the signal decay rate, $P_t^{\rm sig}$, depends on the tagging results q and η. It is modeled by a PDF of the true time $\hat{t}$, $R(\hat{t}, q, \eta)$, convolved with the decay time resolution and multiplied by the decay time acceptance function found for $\overline{B}{}^0 \to J/\psi \overline{K}{}^{*0}$ events. From Eq. (1), it can be expressed as

$$\begin{aligned} R(\hat{t}, q, \eta) \propto e^{-\Gamma_s\hat{t}} \Bigg\{ &\cosh\frac{\Delta\Gamma_s\hat{t}}{2} + \cos\phi_s \sinh\frac{\Delta\Gamma_s\hat{t}}{2} \\ &- q\big[1 - 2\omega(\eta)\big]\sin\phi_s \sin(\Delta m_s\hat{t}) \Bigg\}, \end{aligned} \tag{8}$$

where $\omega(\eta)$ is the calibrated mistag probability. Thus the PDF of reconstructed time is

$$P_t^{\rm sig}(t, q, \eta|\sigma_t) = R(\hat{t}, q, \eta) \otimes T(t-\hat{t};\sigma_t) \cdot A(t; a, n, t_0). \tag{9}$$

For untagged events we use

$$\begin{aligned} &P(m_i, t_i, \sigma_{ti}, q_i = 0, \eta_i) \\ &\quad = N_{\rm sig}(1 - \varepsilon_{\rm tag}) P_m^{\rm sig}(m_i) P_t^{\rm sig}(t_i, 0, \eta_i|\sigma_{ti}) P_{\sigma_t}^{\rm sig}(\sigma_{ti}) \\ &\qquad + N_{\rm bkg}\big(1 - \varepsilon_{\rm tag}^{\rm bkg}\big) P_m^{\rm bkg}(m_i) P_t^{\rm bkg}(t_i|\sigma_{ti}) P_{\sigma_t}^{\rm bkg}(\sigma_{ti}). \end{aligned} \tag{10}$$

The PDF describing the long-lived background decay rate is

$$\begin{aligned} P_t^{\rm bkg}(t|\sigma_t) = &\left[\frac{1 - f_2^{\rm bkg}}{\tau_1^{\rm bkg}} e^{-\frac{\hat{t}}{\tau_1^{\rm bkg}}} + \frac{f_2^{\rm bkg}}{\tau_2^{\rm bkg}} e^{-\frac{\hat{t}}{\tau_2^{\rm bkg}}}\right] \\ &\otimes T(t-\hat{t};\sigma_t) \cdot A\big(t; a^{\rm bkg}, n^{\rm bkg}, t_0^{\rm bkg}\big), \end{aligned} \tag{11}$$

where $\tau_1^{\rm bkg}$, $\tau_2^{\rm bkg}$ and $f_2^{\rm bkg}$ parameterize the underlying double exponential function. The same functional form is used to describe the background decay time acceptance as for signal (Eq. (5)) with different parameters that are determined by fitting the like-sign $J/\psi\pi^\pm\pi^\pm$ events in an interval ± 200 MeV around the $\overline{B}{}_s^0$ mass. The $P_{\sigma_t}^{\rm sig}(\sigma_{ti})$ and $P_{\sigma_t}^{\rm bkg}(\sigma_{ti})$ functions are shown in Fig. 5. The parameters that are fixed in the likelihood fit are listed in Table 3.

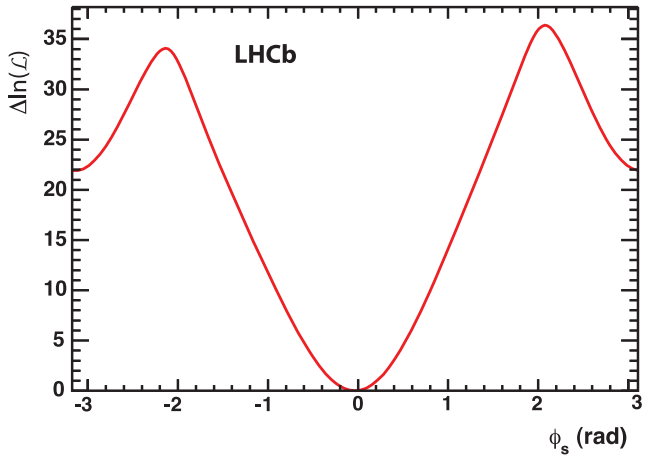

Fig. 8. Log-likelihood difference as a function of ϕ_s for $\overline{B}{}_s^0 \to J/\psi f_{\rm odd}$ events.

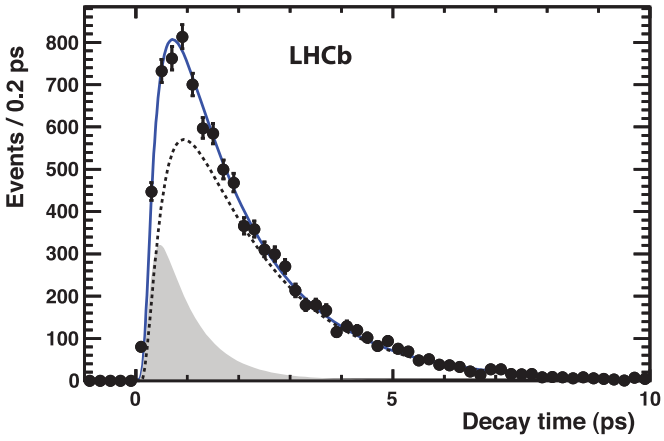

Fig. 9. Decay time distribution of $\overline{B}{}_s^0 \to J/\psi f_{\rm odd}$ candidates. The solid line shows the result of the fit, the dashed line shows the signal, and the shaded region the background.

8. Results

The likelihood of Eq. (6) is multiplied by Gaussian constraints on several of the model parameters. These are the LHCb measured value of $\Delta m_s = 17.63 \pm 0.11 \pm 0.02$ ps^{-1} [20], the tagging parameters p_0 and p_1, the decay time acceptance parameters t_0, a, and n, and both $\Gamma_s = 0.657 \pm 0.009 \pm 0.008$ ps^{-1} and $\Delta\Gamma_s = 0.123 \pm 0.029 \pm 0.011$ ps^{-1} given by the $J/\psi\phi$ analysis [7]. The fit has been validated with full Monte Carlo simulations.

Fig. 8 shows the difference of log-likelihood value, $\Delta\ln(\mathcal{L})$, compared to the one at the point with the best fit, as a function of ϕ_s. At each value, the likelihood function is maximized with respect to all other parameters. The best fit value is $\phi_s = -0.019^{+0.173+0.004}_{-0.174-0.003}$ rad. (The systematic uncertainty will be discussed subsequently.) Values for ϕ_s in the f_0 and $\tilde{f}_0$ regions are -0.26 ± 0.23 rad and 0.29 ± 0.28 rad, respectively, consistent within the uncertainties. The decay time distribution is shown in Fig. 9.

The presence of a $\sin\phi_s$ contribution in Eq. (1) can, in principle, be viewed by plotting the asymmetry $[N(\overline{B}{}_s^0) - N(B_s^0)]/[N(\overline{B}{}_s^0) + N(B_s^0)]$ of the background-subtracted tagged yields as a function of decay time modulo $2\pi/\Delta m_s$, as shown in Fig. 10. The asymmetry is consistent with the value of ϕ_s determined from the full fit and does not show any significant structure.

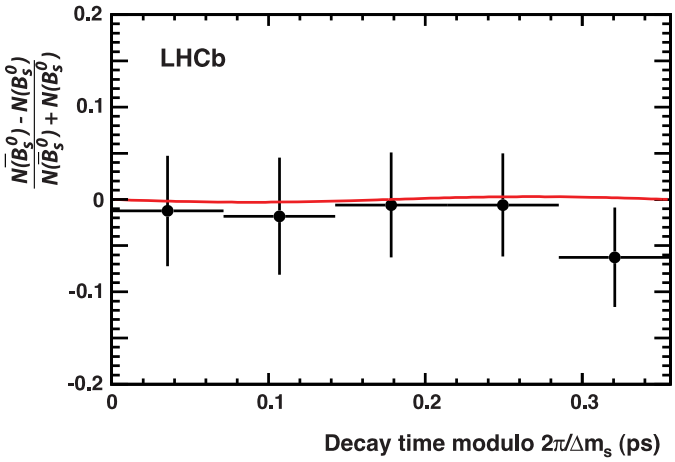

Fig. 10. *CP* asymmetry as a function of decay time modulo $2\pi/\Delta m_s$. The curve shows the expectation for $\phi_s = -0.019$ rad.

The data have also been analyzed allowing for the possibility of direct *CP* violation. In this case Eq. (8) must be replaced with

$$R(\hat{t}, q, \eta) \propto e^{-\Gamma_s \hat{t}} \left\{ \cosh\frac{\Delta\Gamma_s \hat{t}}{2} + \frac{2|\lambda|}{1+|\lambda|^2}\cos\phi_s \sinh\frac{\Delta\Gamma_s \hat{t}}{2} - \frac{q[1-2\omega(\eta)]}{1+|\lambda|^2}\left[2|\lambda|\sin\phi_s \sin(\Delta m_s \hat{t}) - \left(1-|\lambda|^2\right)\cos(\Delta m_s \hat{t})\right] \right\}. \quad (12)$$

The fit gives $|\lambda| = 0.89 \pm 0.13$, consistent with no direct *CP* violation ($|\lambda| = 1$). The value of ϕ_s changes only by -0.002 rad, and the uncertainty stays the same.

The systematic uncertainties are small compared to the statistical one. No additional uncertainty is introduced by the acceptance parameters, Δm_s, Γ_s, $\Delta\Gamma_s$ or flavor tagging, since Gaussian constraints are applied in the fit. The uncertainties associated with the fixed parameters are evaluated by changing them by ± 1 standard deviation from their nominal values and determining the change in the fitted value of ϕ_s. These are listed in Table 4. The uncertainty due to a change in the signal time acceptance function is evaluated by multiplying $A(t; a, n, t_0)$ with a factor $(1 + \beta t)$, and redoing the $\overline{B}^0 \to J/\psi \overline{K}^{*0}$ fit with the $\overline{B}^0$ lifetime fixed to the PDG value. The resulting value of $\beta = (1 \pm 3 \pm 3) \times 10^{-3}$ is then varied by $\pm 4.4 \times 10^{-3}$ to estimate the uncertainty in ϕ_s. An additional uncertainty is included due to a possible *CP*-even component. This has been limited to 2.3% of the total $f_{\rm odd}$ rate at 95% CL, and contributes an uncertainty to ϕ_s as determined by repeating the fit with an additional multiplicative dilution of 0.954. The asymmetry between B_s^0 and $\overline{B}_s^0$ production is believed to be small, and similar to the asymmetry between B^0 and $\overline{B}^0$ production which has been measured by LHCb to be about 1% [21]. The effect of neglecting this production asymmetry is the same as making a relative 1% change in the tagging efficiencies, up for B_s^0 and down for $\overline{B}_s^0$, which has a negligible effect on ϕ_s.

9. Conclusions

Using 1 fb^{-1} of data collected with the LHCb detector, $\overline{B}_s^0 \to J/\psi\pi^+\pi^-$ decays are selected and used to measure the *CP* violating phase ϕ_s. The signal events have an effective decay time resolution of 39.8 fs. The flavor tagging is based on properties of the decay of the other b hadron in the event and has an efficiency times dilution-squared of 2.4%. We perform a fit of the time dependent rates with the $\overline{B}_s^0$ lifetime and the difference in widths of the heavy and light eigenstates used as input. We measure a value of $\phi_s = -0.019^{+0.173+0.004}_{-0.174-0.003}$ rad. This result subsumes our previous measurement obtained with 0.41 fb^{-1} of data [6]. Combining this result with our previous result from $\overline{B}_s^0 \to J/\psi\phi$ decays [7] by performing a joint fit to the data gives a combined LHCb value of $\phi_s = +0.06 \pm 0.12 \pm 0.06$ rad. Our result is consistent with the SM prediction of $-0.0363^{+0.0016}_{-0.0015}$ rad [1]. In addition, we find no evidence for direct *CP* violation.

Table 4
Summary of systematic uncertainties on ϕ_s. Quantities fixed in the fit that are not included here give negligible uncertainties. The total uncertainty is found by adding in quadrature all the positive and negative contributions separately.

Quantity (Q)	$\pm\Delta Q$	+ Change in ϕ_s (rad)	− Change in ϕ_s (rad)
β	4.4×10^{-3}	0.0008	−0.0007
$\tau_1^{\rm bkg}$ (ps)	0.046	−0.0006	0.0014
$\tau_2^{\rm bkg}$ (ps)	0.8	−0.0014	0.0014
$f_2^{\rm bkg}$	0.02	−0.0006	0.0012
$N_{\rm bkg}$	38	0.0009	−0.0001
$N_{\eta'}$	9	0.0006	0.0001
m_0 (MeV)	0.12	0.0012	−0.0004
σ_1^m (MeV)	0.1	−0.0002	0.0008
α	1.1×10^{-4}	0.0003	0.0003
T function	5%	0.0005	0.0005
CP-even	multiply dilution by 0.954	−0.0008	–
Direct *CP*	free in fit	−0.0020	–
Total systematic uncertainty on ϕ_s		$^{+0.004}_{-0.003}$	

Acknowledgements

We express our gratitude to our colleagues in the CERN accelerator departments for the excellent performance of the LHC. We thank the technical and administrative staff at CERN and at the LHCb institutes, and acknowledge support from the National Agencies: CAPES, CNPq, FAPERJ and FINEP (Brazil); CERN; NSFC (China); CNRS/IN2P3 (France); BMBF, DFG, HGF and MPG (Germany); SFI (Ireland); INFN (Italy); FOM and NWO (The Netherlands); SCSR (Poland); ANCS (Romania); MinES of Russia and Rosatom (Russia); MICINN, XuntaGal and GENCAT (Spain); SNSF and SER (Switzerland); NAS Ukraine (Ukraine); STFC (United Kingdom); NSF (USA). We also acknowledge the support received from the ERC under FP7 and the Region Auvergne.

References

[1] CKMfitter group, J. Charles, et al., Phys. Rev. D 84 (2011) 033005, arXiv:1106.4041.
[2] S. Stone, L. Zhang, Phys. Rev. D 79 (2009) 074024, arXiv:0812.2832.
[3] LHCb Collaboration, R. Aaij, et al., Phys. Lett. B 698 (2011) 115, arXiv:1102.0206.
[4] Belle Collaboration, J. Li, et al., Phys. Rev. Lett. 106 (2011) 121802, arXiv:1102.2759;
D0 Collaboration, V.M. Abazov, et al., Phys. Rev. D 85 (2012) 011103, arXiv:1110.4272.
[5] CDF Collaboration, T. Aaltonen, et al., Phys. Rev. D 84 (2011) 052012, arXiv:1106.3682.
[6] LHCb Collaboration, R. Aaij, et al., Phys. Lett. B 707 (2012) 497, arXiv:1112.3056.
[7] LHCb Collaboration, R. Aaij, et al., Phys. Rev. Lett. 108 (2012) 101803, arXiv:1112.3183.

[8] D0 Collaboration, V.M. Abazov, et al., Phys. Rev. D 85 (2012) 032006, arXiv:1109.3166;
CDF Collaboration, T. Aaltonen, et al., Measurement of the *CP*-violating phase β_s in $B_s^0 \to J/\psi\phi$ decays with the CDF II detector, arXiv:1112.1726.
[9] LHCb Collaboration, R. Aaij, et al., Analysis of the resonant components in $\overline{B}{}_s^0 \to J/\psi\pi^+\pi^-$, arXiv:1204.5675, Phys. Rev. D, in press.
[10] S. Faller, R. Fleischer, T. Mannel, Phys. Rev. D 79 (2009) 014005, arXiv:0810.4248;
R. Fleischer, R. Knegjens, G. Ricciardi, Eur. Phys. J. C 71 (2011) 1832, arXiv:1109.1112.
[11] U. Nierste, Three lectures on meson mixing and CKM phenomenology, arXiv:0904.1869;
I.I. Bigi, A. Sanda, Camb. Monogr. Part. Phys. Nucl. Phys. Cosmol. 9 (2000) 1.
[12] LHCb Collaboration, R. Aaij, et al., Phys. Rev. Lett. 108 (2012) 241801, http://dx.doi.org/10.1103/PhysRevLett.108.241801, arXiv:1202.4717.
[13] LHCb Collaboration, A. Alves Jr., et al., JINST 3 (2008) S08005.
[14] Particle Data Group, K. Nakamura, et al., J. Phys. G 37 (2010) 075021.
[15] A. Hoecker, et al., PoS ACAT (2007) 040, arXiv:physics/0703039.
[16] T. Sjöstrand, S. Mrenna, P. Skands, JHEP 0605 (2006) 026, arXiv:hep-ph/0603175.
[17] GEANT4 Collaboration, S. Agostinelli, et al., Nucl. Instrum. Meth. A 506 (2003) 250.
[18] S.M. Flatté, Phys. Lett. B 63 (1976) 228.
[19] LHCb Collaboration, R. Aaij, et al. Opposite-side flavor tagging of B mesons at the LHCb experiment, arXiv:1202.4979 Eur. Phys. J. C, submitted for publication.
[20] LHCb Collaboration, R. Aaij, et al., Phys. Lett. B 709 (2012) 177, arXiv:1112.4311.
[21] LHCb Collaboration, R. Aaij, et al., First evidence of direct *CP* violation in charmless two-body decays of B_s^0 mesons, arXiv:1202.6251.

LHCb Collaboration

R. Aaij [38], C. Abellan Beteta [33,n], B. Adeva [34], M. Adinolfi [43], C. Adrover [6], A. Affolder [49], Z. Ajaltouni [5], J. Albrecht [35], F. Alessio [35], M. Alexander [48], S. Ali [38], G. Alkhazov [27], P. Alvarez Cartelle [34], A.A. Alves Jr. [22], S. Amato [2], Y. Amhis [36], J. Anderson [37], R.B. Appleby [51], O. Aquines Gutierrez [10], F. Archilli [18,35], A. Artamonov [32], M. Artuso [53,35], E. Aslanides [6], G. Auriemma [22,m], S. Bachmann [11], J.J. Back [45], V. Balagura [28,35], W. Baldini [16], R.J. Barlow [51], C. Barschel [35], S. Barsuk [7], W. Barter [44], A. Bates [48], C. Bauer [10], Th. Bauer [38], A. Bay [36], I. Bediaga [1], S. Belogurov [28], K. Belous [32], I. Belyaev [28], E. Ben-Haim [8], M. Benayoun [8], G. Bencivenni [18], S. Benson [47], J. Benton [43], R. Bernet [37], M.-O. Bettler [17], M. van Beuzekom [38], A. Bien [11], S. Bifani [12], T. Bird [51], A. Bizzeti [17,h], P.M. Bjørnstad [51], T. Blake [35], F. Blanc [36], C. Blanks [50], J. Blouw [11], S. Blusk [53], A. Bobrov [31], V. Bocci [22], A. Bondar [31], N. Bondar [27], W. Bonivento [15], S. Borghi [48,51], A. Borgia [53], T.J.V. Bowcock [49], C. Bozzi [16], T. Brambach [9], J. van den Brand [39], J. Bressieux [36], D. Brett [51], M. Britsch [10], T. Britton [53], N.H. Brook [43], H. Brown [49], K. de Bruyn [38], A. Büchler-Germann [37], I. Burducea [26], A. Bursche [37], J. Buytaert [35], S. Cadeddu [15], O. Callot [7], M. Calvi [20,j], M. Calvo Gomez [33,n], A. Camboni [33], P. Campana [18,35], A. Carbone [14], G. Carboni [21,k], R. Cardinale [19,35,i], A. Cardini [15], L. Carson [50], K. Carvalho Akiba [2], G. Casse [49], M. Cattaneo [35], Ch. Cauet [9], M. Charles [52], Ph. Charpentier [35], N. Chiapolini [37], K. Ciba [35], X. Cid Vidal [34], G. Ciezarek [50], P.E.L. Clarke [47,35], M. Clemencic [35], H.V. Cliff [44], J. Closier [35], C. Coca [26], V. Coco [38], J. Cogan [6], P. Collins [35], A. Comerma-Montells [33], A. Contu [52], A. Cook [43], M. Coombes [43], G. Corti [35], B. Couturier [35], G.A. Cowan [36], R. Currie [47], C. D'Ambrosio [35], P. David [8], P.N.Y. David [38], I. De Bonis [4], S. De Capua [21,k], M. De Cian [37], J.M. De Miranda [1], L. De Paula [2], P. De Simone [18], D. Decamp [4], M. Deckenhoff [9], H. Degaudenzi [36,35], L. Del Buono [8], C. Deplano [15], D. Derkach [14,35], O. Deschamps [5], F. Dettori [39], J. Dickens [44], H. Dijkstra [35], P. Diniz Batista [1], F. Domingo Bonal [33,n], S. Donleavy [49], F. Dordei [11], A. Dosil Suárez [34], D. Dossett [45], A. Dovbnya [40], F. Dupertuis [36], R. Dzhelyadin [32], A. Dziurda [23], S. Easo [46], U. Egede [50], V. Egorychev [28], S. Eidelman [31], D. van Eijk [38], F. Eisele [11], S. Eisenhardt [47], R. Ekelhof [9], L. Eklund [48], Ch. Elsasser [37], D. Elsby [42], D. Esperante Pereira [34], A. Falabella [16,14,e], C. Färber [11], G. Fardell [47], C. Farinelli [38], S. Farry [12], V. Fave [36], V. Fernandez Albor [34], M. Ferro-Luzzi [35], S. Filippov [30], C. Fitzpatrick [47], M. Fontana [10], F. Fontanelli [19,i], R. Forty [35], O. Francisco [2], M. Frank [35], C. Frei [35], M. Frosini [17,f], S. Furcas [20], A. Gallas Torreira [34], D. Galli [14,c], M. Gandelman [2], P. Gandini [52], Y. Gao [3], J.-C. Garnier [35], J. Garofoli [53], J. Garra Tico [44], L. Garrido [33], D. Gascon [33], C. Gaspar [35], R. Gauld [52], N. Gauvin [36], M. Gersabeck [35], T. Gershon [45,35], Ph. Ghez [4], V. Gibson [44], V.V. Gligorov [35], C. Göbel [54,p], D. Golubkov [28], A. Golutvin [50,28,35], A. Gomes [2], H. Gordon [52], M. Grabalosa Gándara [33], R. Graciani Diaz [33], L.A. Granado Cardoso [35], E. Graugés [33], G. Graziani [17], A. Grecu [26], E. Greening [52], S. Gregson [44], B. Gui [53], E. Gushchin [30], Yu. Guz [32], T. Gys [35], C. Hadjivasiliou [53], G. Haefeli [36], C. Haen [35], S.C. Haines [44], T. Hampson [43], S. Hansmann-Menzemer [11], R. Harji [50], N. Harnew [52], J. Harrison [51], P.F. Harrison [45], T. Hartmann [55,q], J. He [7], V. Heijne [38], K. Hennessy [49], P. Henrard [5], J.A. Hernando Morata [34], E. van Herwijnen [35], E. Hicks [49], K. Holubyev [11], P. Hopchev [4], W. Hulsbergen [38], P. Hunt [52], T. Huse [49], R.S. Huston [12], D. Hutchcroft [49], D. Hynds [48], V. Iakovenko [41], P. Ilten [12], J. Imong [43], R. Jacobsson [35], A. Jaeger [11], M. Jahjah Hussein [5], E. Jans [38], F. Jansen [38], P. Jaton [36], B. Jean-Marie [7], F. Jing [3], M. John [52], D. Johnson [52], C.R. Jones [44], B. Jost [35], M. Kaballo [9], S. Kandybei [40], M. Karacson [35], T.M. Karbach [9], J. Keaveney [12], I.R. Kenyon [42], U. Kerzel [35], T. Ketel [39], A. Keune [36], B. Khanji [6], Y.M. Kim [47], M. Knecht [36], R.F. Koopman [39], P. Koppenburg [38],

M. Korolev [29], A. Kozlinskiy [38], L. Kravchuk [30], K. Kreplin [11], M. Kreps [45], G. Krocker [11], P. Krokovny [11], F. Kruse [9], K. Kruzelecki [35], M. Kucharczyk [20,23,35,j], V. Kudryavtsev [31], T. Kvaratskheliya [28,35], V.N. La Thi [36], D. Lacarrere [35], G. Lafferty [51], A. Lai [15], D. Lambert [47], R.W. Lambert [39], E. Lanciotti [35], G. Lanfranchi [18], C. Langenbruch [11], T. Latham [45], C. Lazzeroni [42], R. Le Gac [6], J. van Leerdam [38], J.-P. Lees [4], R. Lefèvre [5], A. Leflat [29,35], J. Lefrançois [7], O. Leroy [6], T. Lesiak [23], L. Li [3], L. Li Gioi [5], M. Lieng [9], M. Liles [49], R. Lindner [35], C. Linn [11], B. Liu [3], G. Liu [35], J. von Loeben [20], J.H. Lopes [2], E. Lopez Asamar [33], N. Lopez-March [36], H. Lu [3], J. Luisier [36], A. Mac Raighne [48], F. Machefert [7], I.V. Machikhiliyan [4,28], F. Maciuc [10], O. Maev [27,35], J. Magnin [1], S. Malde [52], R.M.D. Mamunur [35], G. Manca [15,d], G. Mancinelli [6], N. Mangiafave [44], U. Marconi [14], R. Märki [36], J. Marks [11], G. Martellotti [22], A. Martens [8], L. Martin [52], A. Martín Sánchez [7], M. Martinelli [38], D. Martinez Santos [35], A. Massafferri [1], Z. Mathe [12], C. Matteuzzi [20], M. Matveev [27], E. Maurice [6], B. Maynard [53], A. Mazurov [16,30,35], G. McGregor [51], R. McNulty [12], M. Meissner [11], M. Merk [38], J. Merkel [9], S. Miglioranzi [35], D.A. Milanes [13], M.-N. Minard [4], J. Molina Rodriguez [54,p], S. Monteil [5], D. Moran [12], P. Morawski [23], R. Mountain [53], I. Mous [38], F. Muheim [47], K. Müller [37], R. Muresan [26], B. Muryn [24], B. Muster [36], J. Mylroie-Smith [49], P. Naik [43], T. Nakada [36], R. Nandakumar [46], I. Nasteva [1], M. Needham [47], N. Neufeld [35], A.D. Nguyen [36], C. Nguyen-Mau [36,o], M. Nicol [7], V. Niess [5], N. Nikitin [29], A. Nomerotski [52,35], A. Novoselov [32], A. Oblakowska-Mucha [24], V. Obraztsov [32], S. Oggero [38], S. Ogilvy [48], O. Okhrimenko [41], R. Oldeman [15,35,d], M. Orlandea [26], J.M. Otalora Goicochea [2], P. Owen [50], B. Pal [53], J. Palacios [37], A. Palano [13,b], M. Palutan [18], J. Panman [35], A. Papanestis [46], M. Pappagallo [48], C. Parkes [51], C.J. Parkinson [50], G. Passaleva [17], G.D. Patel [49], M. Patel [50], S.K. Paterson [50], G.N. Patrick [46], C. Patrignani [19,i], C. Pavel-Nicorescu [26], A. Pazos Alvarez [34], A. Pellegrino [38], G. Penso [22,l], M. Pepe Altarelli [35], S. Perazzini [14,c], D.L. Perego [20,j], E. Perez Trigo [34], A. Pérez-Calero Yzquierdo [33], P. Perret [5], M. Perrin-Terrin [6], G. Pessina [20], A. Petrolini [19,i], A. Phan [53], E. Picatoste Olloqui [33], B. Pie Valls [33], B. Pietrzyk [4], T. Pilař [45], D. Pinci [22], R. Plackett [48], S. Playfer [47], M. Plo Casasus [34], G. Polok [23], A. Poluektov [45,31], E. Polycarpo [2], D. Popov [10], B. Popovici [26], C. Potterat [33], A. Powell [52], J. Prisciandaro [36], V. Pugatch [41], A. Puig Navarro [33], W. Qian [53], J.H. Rademacker [43], B. Rakotomiaramanana [36], M.S. Rangel [2], I. Raniuk [40], G. Raven [39], S. Redford [52], M.M. Reid [45], A.C. dos Reis [1], S. Ricciardi [46], A. Richards [50], K. Rinnert [49], D.A. Roa Romero [5], P. Robbe [7], E. Rodrigues [48,51], F. Rodrigues [2], P. Rodriguez Perez [34], G.J. Rogers [44], S. Roiser [35], V. Romanovsky [32], M. Rosello [33,n], J. Rouvinet [36], T. Ruf [35], H. Ruiz [33], G. Sabatino [21,k], J.J. Saborido Silva [34], N. Sagidova [27], P. Sail [48], B. Saitta [15,d], C. Salzmann [37], M. Sannino [19,i], R. Santacesaria [22], C. Santamarina Rios [34], R. Santinelli [35], E. Santovetti [21,k], M. Sapunov [6], A. Sarti [18,l], C. Satriano [22,m], A. Satta [21], M. Savrie [16,e], D. Savrina [28], P. Schaack [50], M. Schiller [39], H. Schindler [35], S. Schleich [9], M. Schlupp [9], M. Schmelling [10], B. Schmidt [35], O. Schneider [36], A. Schopper [35], M.-H. Schune [7], R. Schwemmer [35], B. Sciascia [18], A. Sciubba [18,l], M. Seco [34], A. Semennikov [28], K. Senderowska [24], I. Sepp [50], N. Serra [37], J. Serrano [6], P. Seyfert [11], M. Shapkin [32], I. Shapoval [40,35], P. Shatalov [28], Y. Shcheglov [27], T. Shears [49], L. Shekhtman [31], O. Shevchenko [40], V. Shevchenko [28], A. Shires [50], R. Silva Coutinho [45], T. Skwarnicki [53], N.A. Smith [49], E. Smith [52,46], K. Sobczak [5], F.J.P. Soler [48], A. Solomin [43], F. Soomro [18,35], B. Souza De Paula [2], B. Spaan [9], A. Sparkes [47], P. Spradlin [48], F. Stagni [35], S. Stahl [11], O. Steinkamp [37], S. Stoica [26], S. Stone [53,35,*], B. Storaci [38], M. Straticiuc [26], U. Straumann [37], V.K. Subbiah [35], S. Swientek [9], M. Szczekowski [25], P. Szczypka [36], T. Szumlak [24], S. T'Jampens [4], E. Teodorescu [26], F. Teubert [35], C. Thomas [52], E. Thomas [35], J. van Tilburg [11], V. Tisserand [4], M. Tobin [37], S. Topp-Joergensen [52], N. Torr [52], E. Tournefier [4,50], S. Tourneur [36], M.T. Tran [36], A. Tsaregorodtsev [6], N. Tuning [38], M. Ubeda Garcia [35], A. Ukleja [25], U. Uwer [11], V. Vagnoni [14], G. Valenti [14], R. Vazquez Gomez [33], P. Vazquez Regueiro [34], S. Vecchi [16], J.J. Velthuis [43], M. Veltri [17,g], B. Viaud [7], I. Videau [7], D. Vieira [2], X. Vilasis-Cardona [33,n], J. Visniakov [34], A. Vollhardt [37], D. Volyanskyy [10], D. Voong [43], A. Vorobyev [27], H. Voss [10], R. Waldi [55,q], S. Wandernoth [11], J. Wang [53], D.R. Ward [44], N.K. Watson [42], A.D. Webber [51], D. Websdale [50], M. Whitehead [45], D. Wiedner [11], L. Wiggers [38], G. Wilkinson [52], M.P. Williams [45,46], M. Williams [50], F.F. Wilson [46], J. Wishahi [9], M. Witek [23], W. Witzeling [35], S.A. Wotton [44], K. Wyllie [35], Y. Xie [47], F. Xing [52], Z. Xing [53], Z. Yang [3], R. Young [47], O. Yushchenko [32], M. Zangoli [14], M. Zavertyaev [10,a], F. Zhang [3], L. Zhang [53], W.C. Zhang [12], Y. Zhang [3], A. Zhelezov [11], L. Zhong [3], A. Zvyagin [35]

[1] *Centro Brasileiro de Pesquisas Físicas (CBPF), Rio de Janeiro, Brazil*
[2] *Universidade Federal do Rio de Janeiro (UFRJ), Rio de Janeiro, Brazil*
[3] *Center for High Energy Physics, Tsinghua University, Beijing, China*

[4] LAPP, Université de Savoie, CNRS/IN2P3, Annecy-Le-Vieux, France
[5] Clermont Université, Université Blaise Pascal, CNRS/IN2P3, LPC, Clermont-Ferrand, France
[6] CPPM, Aix-Marseille Université, CNRS/IN2P3, Marseille, France
[7] LAL, Université Paris-Sud, CNRS/IN2P3, Orsay, France
[8] LPNHE, Université Pierre et Marie Curie, Université Paris Diderot, CNRS/IN2P3, Paris, France
[9] Fakultät Physik, Technische Universität Dortmund, Dortmund, Germany
[10] Max-Planck-Institut für Kernphysik (MPIK), Heidelberg, Germany
[11] Physikalisches Institut, Ruprecht-Karls-Universität Heidelberg, Heidelberg, Germany
[12] School of Physics, University College Dublin, Dublin, Ireland
[13] Sezione INFN di Bari, Bari, Italy
[14] Sezione INFN di Bologna, Bologna, Italy
[15] Sezione INFN di Cagliari, Cagliari, Italy
[16] Sezione INFN di Ferrara, Ferrara, Italy
[17] Sezione INFN di Firenze, Firenze, Italy
[18] Laboratori Nazionali dell'INFN di Frascati, Frascati, Italy
[19] Sezione INFN di Genova, Genova, Italy
[20] Sezione INFN di Milano Bicocca, Milano, Italy
[21] Sezione INFN di Roma Tor Vergata, Roma, Italy
[22] Sezione INFN di Roma La Sapienza, Roma, Italy
[23] Henryk Niewodniczanski Institute of Nuclear Physics Polish Academy of Sciences, Kraków, Poland
[24] AGH University of Science and Technology, Kraków, Poland
[25] Soltan Institute for Nuclear Studies, Warsaw, Poland
[26] Horia Hulubei National Institute of Physics and Nuclear Engineering, Bucharest-Magurele, Romania
[27] Petersburg Nuclear Physics Institute (PNPI), Gatchina, Russia
[28] Institute of Theoretical and Experimental Physics (ITEP), Moscow, Russia
[29] Institute of Nuclear Physics, Moscow State University (SINP MSU), Moscow, Russia
[30] Institute for Nuclear Research of the Russian Academy of Sciences (INR RAN), Moscow, Russia
[31] Budker Institute of Nuclear Physics (SB RAS) and Novosibirsk State University, Novosibirsk, Russia
[32] Institute for High Energy Physics (IHEP), Protvino, Russia
[33] Universitat de Barcelona, Barcelona, Spain
[34] Universidad de Santiago de Compostela, Santiago de Compostela, Spain
[35] European Organization for Nuclear Research (CERN), Geneva, Switzerland
[36] Ecole Polytechnique Fédérale de Lausanne (EPFL), Lausanne, Switzerland
[37] Physik-Institut, Universität Zürich, Zürich, Switzerland
[38] Nikhef National Institute for Subatomic Physics, Amsterdam, The Netherlands
[39] Nikhef National Institute for Subatomic Physics and Vrije Universiteit, Amsterdam, The Netherlands
[40] NSC Kharkiv Institute of Physics and Technology (NSC KIPT), Kharkiv, Ukraine
[41] Institute for Nuclear Research of the National Academy of Sciences (KINR), Kyiv, Ukraine
[42] University of Birmingham, Birmingham, United Kingdom
[43] H.H. Wills Physics Laboratory, University of Bristol, Bristol, United Kingdom
[44] Cavendish Laboratory, University of Cambridge, Cambridge, United Kingdom
[45] Department of Physics, University of Warwick, Coventry, United Kingdom
[46] STFC Rutherford Appleton Laboratory, Didcot, United Kingdom
[47] School of Physics and Astronomy, University of Edinburgh, Edinburgh, United Kingdom
[48] School of Physics and Astronomy, University of Glasgow, Glasgow, United Kingdom
[49] Oliver Lodge Laboratory, University of Liverpool, Liverpool, United Kingdom
[50] Imperial College London, London, United Kingdom
[51] School of Physics and Astronomy, University of Manchester, Manchester, United Kingdom
[52] Department of Physics, University of Oxford, Oxford, United Kingdom
[53] Syracuse University, Syracuse, NY, United States
[54] Pontifícia Universidade Católica do Rio de Janeiro (PUC-Rio), Rio de Janeiro, Brazil
[55] Physikalisches Institut, Universität Rostock, Rostock, Germany

* Corresponding author at: Syracuse University, Syracuse, NY, United States.
E-mail address: stone@physics.syr.edu (S. Stone).
[a] P.N. Lebedev Physical Institute, Russian Academy of Science (LPI RAS), Moscow, Russia.
[b] Università di Bari, Bari, Italy.
[c] Università di Bologna, Bologna, Italy.
[d] Università di Cagliari, Cagliari, Italy.
[e] Università di Ferrara, Ferrara, Italy.
[f] Università di Firenze, Firenze, Italy.
[g] Università di Urbino, Urbino, Italy.
[h] Università di Modena e Reggio Emilia, Modena, Italy.
[i] Università di Genova, Genova, Italy.
[j] Università di Milano Bicocca, Milano, Italy.
[k] Università di Roma Tor Vergata, Roma, Italy.
[l] Università di Roma La Sapienza, Roma, Italy.
[m] Università della Basilicata, Potenza, Italy.
[n] LIFAELS, La Salle, Universitat Ramon Llull, Barcelona, Spain.
[o] Hanoi University of Science, Hanoi, Viet Nam.
[p] Associated to Universidade Federal do Rio de Janeiro (UFRJ), Rio de Janeiro, Brazil.
[q] Associated to Physikalisches Institut, Ruprecht-Karls-Universität Heidelberg, Heidelberg, Germany.